Identification of high explosive RDX using terahertz imaging and spectral fingerprints

Jia Liu[1,2], Wen-Hui Fan*[,1], Xu Chen[1,2] and Jun Xie[1,2]

[1]State Key Laboratory of Transient Optics and Photonics, Xi'an Institute of Optics and Precision Mechanics, Chinese Academy of Sciences, Xi'an 710119, China

[2]Graduate University of Chinese Academy of Sciences, Beijing 100049, China

E-mail: fanwh@opt.ac.cn

Abstract. We experimentally investigated the spectral fingerprints of high explosive cyclo-1,3,5-trimethylene-2,4,6-trinitramine (RDX) in terahertz frequency region. A home-made terahertz time-domain spectroscopy ranging from 0.2 THz～3.4 THz was deployed. Furthermore, two sample pellets (RDX pellet and polyethylene pellet), which were concealed in an opaque envelop, could be identified by using terahertz pulse imaging system. For the purpose of distinguishing the RDX between two pellets, we further calculated the THz frequency-domain map using its spectral fingerprints. It is demonstrated that the high explosive RDX could similarly be identified using terahertz frequency-domain imaging.

1. Introduction

Over the past several years, terrorist attacks have been substantially increasing worldwide. For example, mail-bombs, anthrax hidden in envelops and concealed metallic or non-metallic (ceramic, fiberglass, plastic) weapon threaten people's daily life. Counter-terrorist has become a significant mission of local government in every country. Hence, a rapid detection and effective identification are needed. Terahertz spectroscopy and imaging have been identified as very promising techniques in a wide area of security applications, such as chemical identification [1-2], imaging of concealed weapon [3-4], biological agent [5-6], and the detection of illicit drugs [7-8] and explosives [9-12].

Terahertz frequency radiation allows for non-destructive and non-invasive inspection of most opaque barrier materials, such as cardboard, wood, plastic, leathern, and textile [13-15]. Many solid-state explosives exhibit distinctive absorption characteristics in THz frequency [16-20]. Each explosive has its own spectral fingerprint, which is essential in the process of identifying the unknown target. These spectral fingerprints arise from the intramolecular and intermolecular vibrational modes or photon modes of the materials.

This paper was experimentally investigated that the high explosive cyclo-1,3,5-trimethylene-2,4,6-trinitramine (RDX) could be identified using terahertz imaging and spectral fingerprints. A home-made terahertz time-domain spectroscopy (THz-TDS) was deployed to measure the spectral fingerprints of RDX in the range from 0.2THz to 3.4THz. It could be clearly observed that the RDX

has the absorption features at 0.80THz, 1.05THz, 1.30 and 1.91THz respectively. Furthermore, a sample consisting of the RDX and high density polyethylene (PE) pellets, which are mounted side by side in an opaque envelop, was imaged using terahertz pulse imaging system. For the purpose of identifying the high explosive RDX pellet, we further calculated the THz frequency-domain map using its spectral fingerprints. It was well demonstrated that the high explosive RDX could be distinguished between the two pellets by using terahertz frequency-domain imaging.

2. Experimental setup

A home-made terahertz time-domain spectroscopy (THz-TDS) we deployed in experiments is shown in Figure 1. THz pulses are generated by the Ti: Sapphire oscillator (Spectra Physics) with pulse duration of 20fs, repetition rate of 76MHz, and average power of 600 mW. The laser beam is splited into two beams by a splitter, one for exciting the 0.5mm thick low temperature-grown GaAs photoconductive antenna (emitter), and the other for measuring the THz signal at 1mm thick <110> ZnTe crystal (detector). The emitted THz pulses are collimated and focused by a pair of off-axis parabolic mirrors. The sample is placed right at the THz focus point, perpendicular to the incident THz beam. The transmitted THz beam is collected and focused by using the other pair of off-axis parabolic mirrors onto ZnTe crystal, in which the probe beam detected the THz field by electro-optic sampling (EOS) [21]. To avoid the absorption of water vapor, the THz radiation region is purged by dry air. The THz spectrum without passing through samples is obtained by applying the fast Fourier transform to THz waveform in the ranging of 0.2 THz～3.4 THz, which is shown in Figure 2.

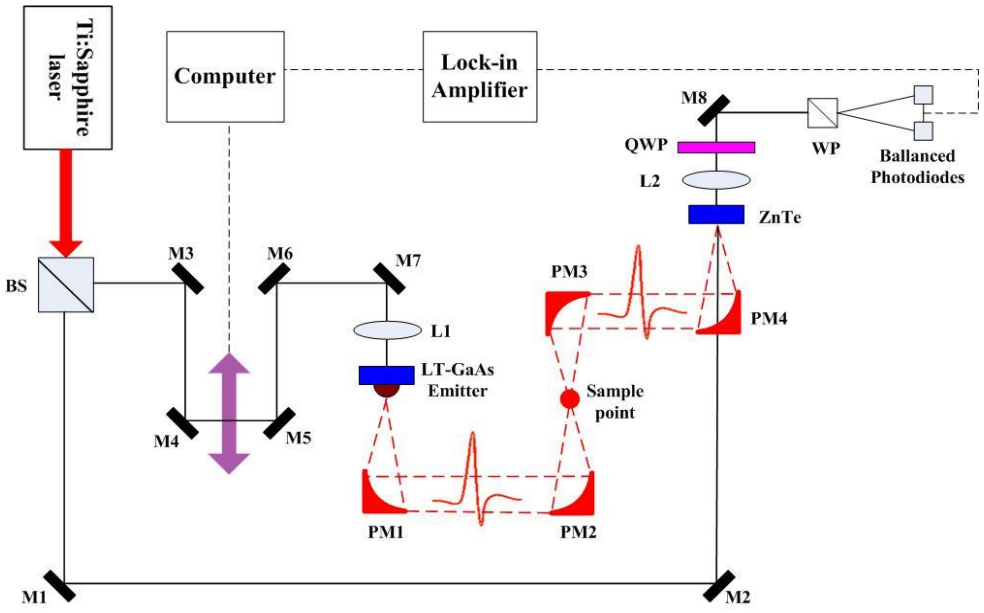

Figure 1. The schematic setup of home-made THz-TDS; BS is beam splitter, M1-M8 is optical mirror, PM1-PM4 is off-axis parabolic mirror, L1-L2 is optical lens, QWP is quarter wave plate, and WP is Wollaston prism.

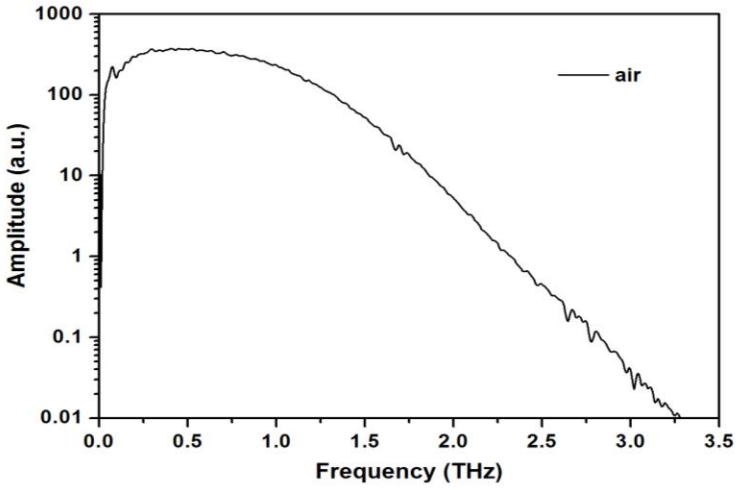

Figure 2. The THz spectrum without passing through samples in dry air.

3. Terahertz Spectra

3.1 Theoretical background

Unlike others spectroscopy, THz-TDS can use to measure the spectra of the explosive related compounds because a single measurement of THz electric field can provide both the amplitude and phase information. Hence, the THz-TDS is capable of obtaining the absorption coefficient and the refractive index without using Kramers-Kronig (K-K) relation [22]. The field of transmitted THz pulse is changed by the dispersion and absorption of sample. The amplitude transmittance of THz field can be described as Eq. (1) [23]:

$$T = \frac{\tilde{E}_{sam}(\upsilon)}{\tilde{E}_{ref}(\upsilon)} = Ae^{i\varphi} = \frac{4\tilde{n}(\upsilon)}{[1+\tilde{n}(\upsilon)]^2} \cdot \left\{ 1 + \frac{[\tilde{n}(\upsilon)-1]^2}{[\tilde{n}(\upsilon)+1]^2} e^{i2\tilde{n}(\upsilon)\upsilon d/c} \right\}^{-1} e^{i2\pi[\tilde{n}(\upsilon)-1]\upsilon d/c} \quad (1)$$

Where $\tilde{E}_{sam}(\upsilon)$ and $\tilde{E}_{ref}(\upsilon)$ are the THz transmitted field and the incident field respectively; A is the amplitude of THz transmitted field; φ is the phase difference between sample and reference waveform; $\tilde{n}(\upsilon) = n(\upsilon) + i\kappa(\upsilon)$ is the complex refractive index; d is the thickness of sample; υ is the frequency of THz field radiation; $\kappa(\upsilon)$ is the extinction coefficient; c is the speed of light in vacuum. In the condition of $\kappa(\upsilon) << n(\upsilon)$, the multiple internal refraction and the Fabry-Perot effect can be neglected. Hence the refractive index $n(\upsilon)$ and extinction coefficient $\kappa(\upsilon)$ can be obtained after a single measurement [24]:

$$n(\upsilon) = \frac{c\varphi}{2\pi d\upsilon} + 1 \quad (2)$$

$$\kappa(\upsilon) = \frac{c}{2\pi d\upsilon} \ln\left(\frac{4n}{A(1+n)^2}\right) \quad (3)$$

Refer to Eq. (2) and Eq. (3), the absorption coefficient can be calculated as Eq. (4):

$$\alpha(\upsilon) = \frac{4\pi\upsilon\kappa(\upsilon)}{c} = \frac{2}{d}\ln\left\{\frac{4n(\upsilon)}{A[1+n(\upsilon)]^2}\right\} \tag{4}$$

Therefore, after measuring the THz transmitted field $\tilde{E}_{sam}(\upsilon)$, the incident field $\tilde{E}_{ref}(\upsilon)$ and the thickness of sample *d*, the refractive index and absorption coefficient can be obtained.

3.2 Sample preparation

The samples of the high explosive RDX (purity > 99%) used in experiments are powder samples. In order to eliminated the influence of scattering, the sample are crash into fine powders using mortar and pestle to reduce the particle size less than 80μm. Considering that the RDX is sensitive and unsafe to high pressure, we mix the RDX with high density polyethylene (PE) which is transparent in THz frequency region. The mixing ratio is about 1:5 (40mg RDX vs. 200mg PE). Then, the RDX/PE samples are compressed into pellets with the thickness of 1.5mm and diameter of 13mm under the pressure of 1 ton.

3.3 Results and discussions

As shown in Figure 3, the fast Fourier Transform (FFT) amplitudes of THz time-domain waveform transmitting through the RDX/PE (sample) and pure PE pellets (reference) were obtained. In order to eliminate the influence of the sample surface effects, we measured at least five different spot on the surface of pellet. The data of the spectra we obtained were the average of five spot with 1800 scans at each spot. It is clearly observed that the FFT amplitude of THz filed is dropped down dramatically due to the strong absorption of RDX, especially at about 0.8 THz.

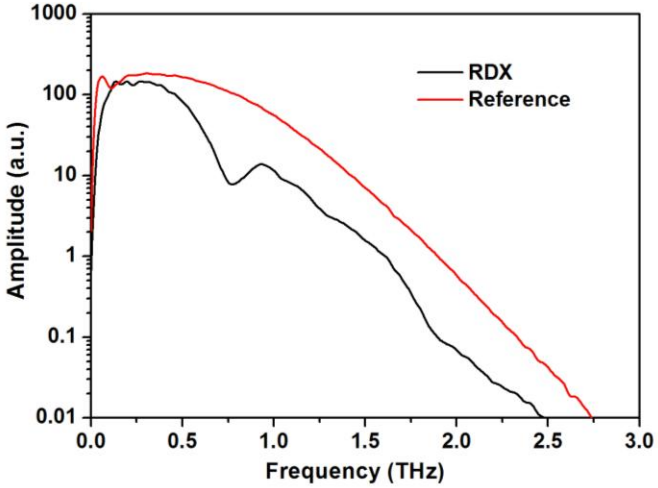

Figure 3. The spectra of THz field transmitted through the RDX/PE pellet and pure PE pellet (reference), respectively.

In order to calculate the absorption coefficient of RDX, we compressed the pure PE powder into pellets, which are taken as the reference. These PE pellets have the same size like the RDX/PE pellets. The absorption spectrum of RDX is calculated using Eq. (2), Eq. (3) and Eq. (4), which is plotted in

Figure 4. It is shown that the RDX has a strong absorption at 0.8 THz and three other relative weak absorptions at 1.05THz, 1.30THz, 1.91THz respectively. This result agrees well with the previous researches [25-26]. Hence, we can easily identify the high explosive RDX using THz spectra fingerprints.

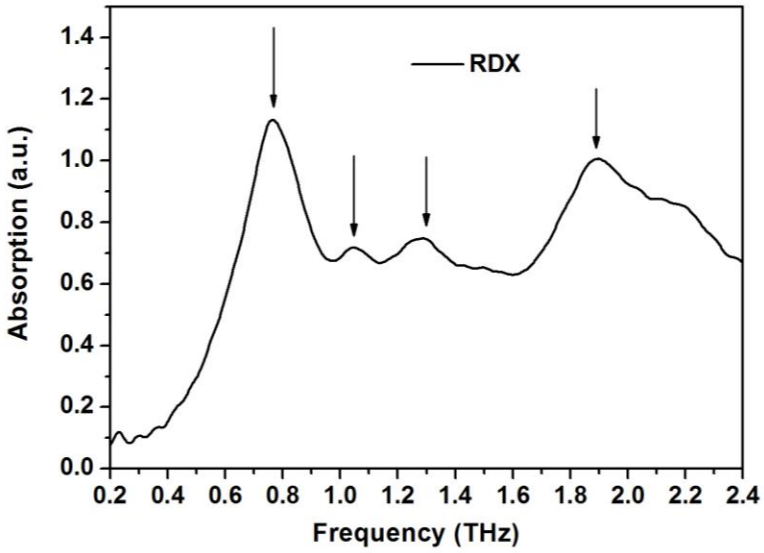

Figure 4. The absorption spectrum of RDX in THz frequency-domain.

4. Terahertz Imaging

Terahertz radiation can penetrate most of non-polarization materials, including cardboard, wood, plastic, leathern, and textile. Hence, terahertz imaging has been identified as a very promising technique in a wide area of security applications, especially for detecting explosive hidden in opaque package. Recently, terahertz imaging using peak-to-peak value of terahertz time-domain waveform is commonly used in nondestructive detection.

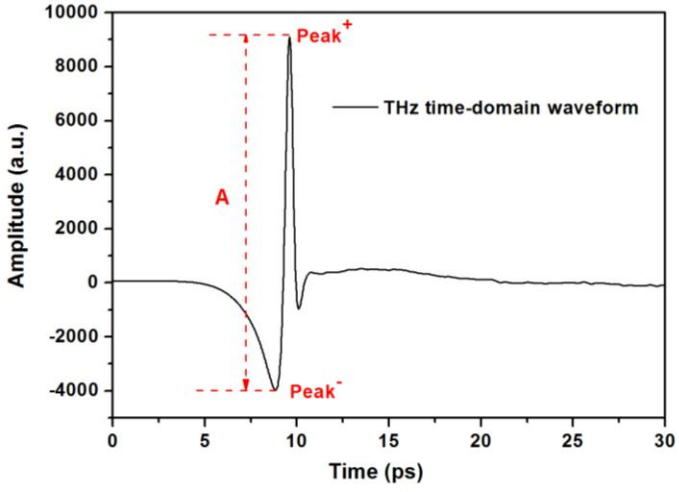

Figure 5. The terahertz time-domain waveform, where $Peak^{+}$ and $Peak^{-}$ are the maximum and minimum value of waveform.

Figure 5 shows the terahertz time-domain waveform obtained in experiments. The amplitude *A* of peak-to-peak value can be calculated by Eq. (5):

$$A = \left| Peak^{+} - Peak^{-} \right| \tag{5}$$

As shown in Figure 6(a), the RDX/PE and pure PE pellets mounted side by side were concealed in an opaque envelop. Both the two pellets have the same size in geometry: 13mm diameter and 1.5mm thickness. Figure 6(b) show the measured terahertz map using peak-to-peak value of terahertz time-domain waveform. The sample was fixed at the THz radiation focus and the map was obtained by raster scanning the THz transmission. The scanned area was 30mm×18mm, which corresponds to 120 pixels×72 pixels with 0.25mm spacing. Each pixel of terahertz map used the calculated value *A* of terahertz time-domain waveform passing through the imaging object. It is clearly observed that the two "invisible" pellets concealed in envelop can be detected by terahertz time-domain imaging. The bright two circles in map are much caused by edge scattering effects [27].

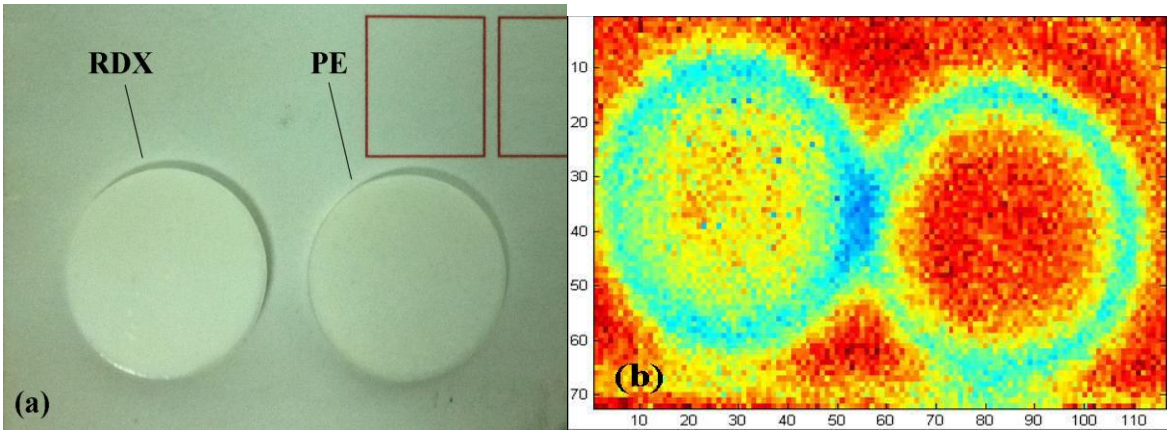

Figure 6. The image of samples concealed in envelop: (a) the photograph of RDX and PE pellets; (b) the false-color THz time-domain image with peak-to-peak amplitude.

From the false-color THz time-domain image alone, it was well demonstrated that the RDX and PE pellets concealed in opaque envelop could be detected by using THz time-domain imaging. However, it couldn't tell which one is the high explosive RDX or the safe PE pellet. For the purpose of identifying the RDX, we further imaged the sample in frequency-domain using its spectral fingerprints. We firstly Fourier transformed the time-domain waveform of each pixel in THz time-domain map. Here we took the THz waveform passing through the hollow envelop as the reference. Refer to Eq. (1)~Eq. (3), the refractive index $n(\upsilon)$ and extinction coefficient $\kappa(\upsilon)$ were calculated. Finally, the THz frequency-domain imaging using the absorption spectra could be obtained. Figure 7(a) shows the process chart of calculated absorption coefficient $\alpha_{i,j}$ responding to the grey scale of each pixel in THz map, and Figure 7(b) shows the calculated THz frequency-domain map using the absorption coefficient at $\upsilon=0.80$ THz. It is clear that only one pellet (left) in Figure 7 (b) can be observed and this circular area has a great absorption. Because high explosive RDX has a strong absorption at 0.8THz, while PE not. It was well demonstrated that the high explosive RDX could be easily distinguished

between the two pellets by using the terahertz frequency-domain imaging.

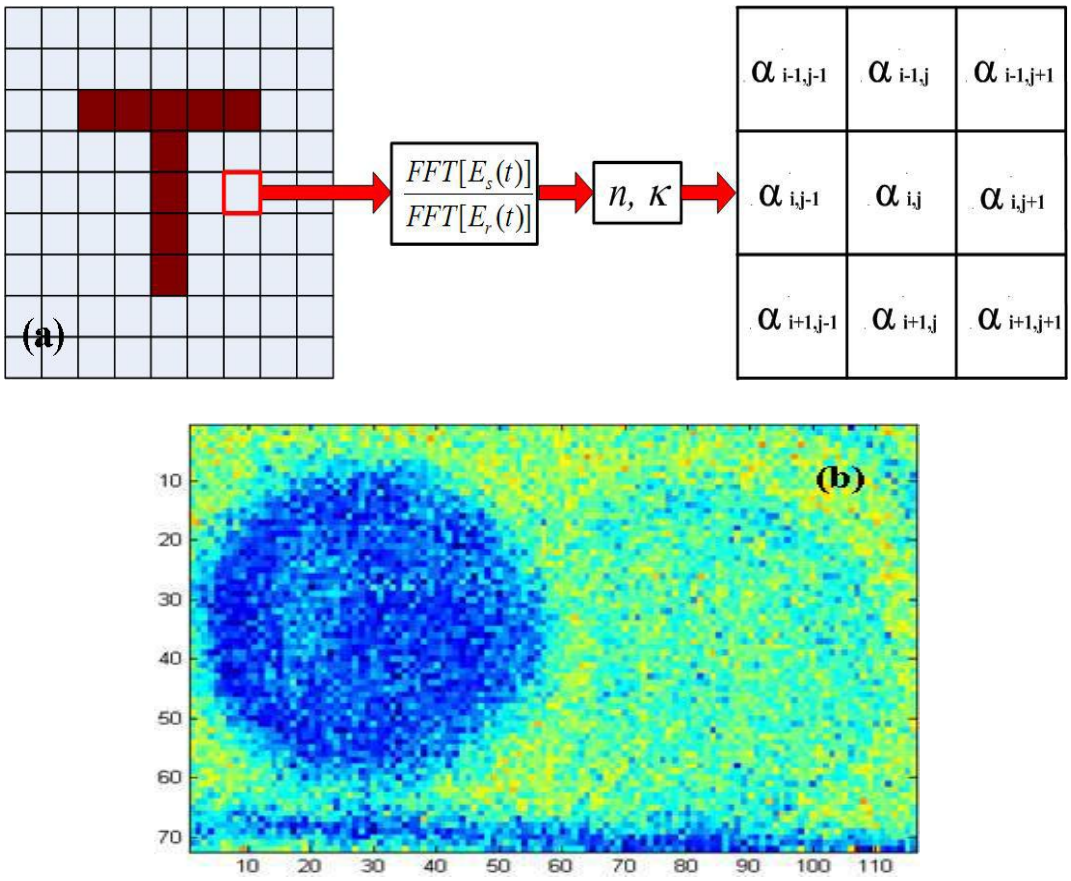

Figure 7. Terahertz frequency-domain imaging: (a) the process chart of calculated absorption coefficient $\alpha_{i,j}$ responding to the grey scale of each pixel in THz map; (b) THz frequency-domain map using the absorption coefficient at υ=*0.80* THz.

5. Conclusion

We experimentally investigated the spectra fingerprints of the high explosive RDX in terahertz frequency region. A home-made terahertz time-domain spectroscopy in the range of 0.2THz～3.4THz was deployed. It is clearly observed that the RDX has a strong absorption at 0.8 THz and three other relative weak absorptions at 1.05THz, 1.30, 1.91THz respectively. Furthermore, a sample consisting of the RDX/PE and pure PE pellets concealed in the opaque envelop, was imaged by using THz pulse system. For the purpose of distinguishing the RDX between the two pellets, we further calculated the THz frequency-domain map using its spectral fingerprints. It is clearly observed that only the RDX pellet can be observed at υ=*0.80* THz. This result well demonstrates that the high explosive RDX could similarly be identified by using the terahertz frequency-domain imaging.

6. References

[1] Jackson J B, Mourou M, Whitaker J F, Duling III I N, Williamson S L, Menu M and Mourou G

A 2008 Terahertz imaging for non-destructive evaluation of mural paintings *Optics Communications* **281** 527

[2] Adam A J L, Planken P C M, Meloni S and Dik J 2009 TeraHertz imaging of hidden paint layers on canvas *Opt. Exp.***17** 3407

[3] Zimdars D and White J S 2004 Terahertz reflection imaging for package and personnel inspection *Proc. of SPIE* **5411** 78

[4] Creeden D, McCarthy J C, Ketteridge P A, Schunemann P G, Southward T, Komiak J J and Chicklis E P 2007 Compact, high average power, fiber-pumped terahertz source for active real-time imaging of concealed objects *Opt. Exp.***15** 6478

[5] Hoshina H, Hayashi A, Miyoshi N, Miyamaru F and Otani C 2009 Terahertz pulsed imaging of frozen biological tissues *Applied Physics Letters* **94** 123901

[6] Fischer B M, Hoffmann M, Helm H, Wilk R, Rutz F, Kleine-Ostmann T, Koch M and Jepsen P U 2005 Terahertz time-domain spectroscopy and imaging of artificial RNA *Opt. Exp.***13** 5205

[7] Kawase K, Ogawa Y and Watanabe Y 2003 Non-destructive terahertz imaging of illicit drugs using spectral fingerprints *Opt. Exp.***11** 2549

[8] Lu M H, Shen J L, Li N, Zhang Y, Zhang C L, Liang L S and Xu X Y 2006 Detection and identification of illicit drugs using terahertz imaging *Journal of Applied Physics* **100** 103104

[9] Davies A G, Burnett A D, Fan W H, Linfield E H and Cunningham J E 2008 Terahertz spectroscopy of explosives and drugs *Materials Today* **11** 18

[10] Fan W H, Burnett A, Upadhya P C, Cunningham J E, Linfield E H and Davies A G 2007 Far-Infrared Spectroscopic Characterization of Explosives for Security Applications Using Broadband Terahertz Time-Domain Spectroscopy *Applied Spectroscopy* **61** 638

[11] Yamamoto K, Yamaguchi M, Miyamaru F, Tani M, Hangyo M, Ikeda T, Matsushita A, Koide K, Tatsuno M and Minami Y 2004 Noninvasive inspection of C-4 explosive in mails by terahertz time-domain spectroscopy *Jpn. J. Appl. Phys.* **43** 414

[12] Shen Y C, Lo T, Taday P F, Cole B E, Tribe W R and Kemp M C 2005 Detection and identification of explosives using terahertz pulsed spectroscopic imaging *Appl. Phys. Lett.* **86** 241116

[13] Bjarnason J E, Chan T L J, Lee A W M, Celis M A and Brown E R 2004 Millimeter-wave, terahertz, and mid-infrared transmission through common clothing 2004 *Applied Physics Letters* **58** 519

[14] Morita Y, Dobroiu A, Kawase K and Otani C 2005 Terahertz technique for detection of microleaks in the seal of flexible plastic packages Optical Engineering **44** 019001

[15] Dunayevskiy I, Bortnik B, Geary K, Lombardo R, Jack M and Fetterman H 2007 Millimeter- and submillimeter-wave characterization of various fabrics *Applied Optics* **46** 6161

[16] Liu H B, Chen Y Q, Bastiaans G J and Zhang X C 2006 Detection and identification of explosive RDX by THz diffuse reflection spectroscopy *Opt. Exp.* **14** 415

[17] Hooper J, Mitchell E, Konek C and Wilkinson J 2009 Terahertz optical properties of the high explosive b-HMX *Chemical Physics Letters* **467** 309

[18] Konek C, Wilkinson J, Esenturk O, Heilweil E and Kemp M 2009 Terahertz Spectroscopy of Explosives and Simulants – RDX, PETN, Sugar and L-Tartaric Acid *Proc. of SPIE* **7311**

73110K
[19] Allis D G, Hakey P M and Korter T M 2008 The solid-state terahertz spectrum of MDMA (Ecstasy)–A unique test for molecular modeling assignments *Chemical Physics Letters* **463** 353
[20] Chen J, Chen Y Q, Zhao H W, Bastiaans G J and Zhang X C 2007 Absorption coefficients of selected explosives and related compounds in the range of 0.1-2.8 THz *Opt. Exp*.**15** 12060
[21] Wu Q, Litz M and Zhang X C 1996 Broadband detection capability of ZnTe electro-optic field detectors *Appl. Phys. Lett.* **68** 2924
[22] Chen Y, Liu H, Deng Y, Schauki D, Fitch M J, Osiander R, Dodson C, Spicer J B, Shur M and Zhang X C 2004 THz spectroscopic investigation of 2,4-dinitrotoluene *Chem. Phys. Lett.* **400** 357
[23] Born M and Wolf E 1964 *Principles of Optics, 2ed* (Oxford: Pergamon Press)
[24] Hu Y, Huang P, Guo L T, Wang X H and Zhang C L 2006 Terahertz spectroscopic investigations of explosives *Physics Letters A* **359** 728
[25] Fitch M J, Leahy-Hoppa M R, Ott E W and Osiander R 2007 Molecular absorption cross-section and absolute absorptivity in the THz frequency range for the explosives TNT, RDX, HMX, and PETN *Chem. Phys. Lett.***443** 284
[26] Huang F, Schulkin B, Altan H, Federici J F, Gary D, Barat R, Zimdars D, Chen M H and Tanner D B 2004 Terahertz study of 1,3,5-trinitro-s-triazine by time-domain and Fourier transform infrared spectroscopy *Applied Physics Letters* **85** 55535
[27] Zhang Z W, Zhang Y, Zhao G Z and Zhang C L 2007 Terahertz time-domain spectroscopy for explosive imaging *Optik* **118** 325

Acknowledgements
This work was supported by the Hundred Talent Program of the Chinese Academy of Sciences (Grant No. J08-029), the Main Direction Program of Knowledge Innovation of the Chinese Academy of Sciences (Grant No. YYYJ-1123-4), the National High Technology Research and Development Program of China (Grant No. 2011AAxxx2008A), the National Basic Research Program of China (Grant No. 2007CB310405) and the CAS/SAFEA International Partnership Program for Creative Research Teams.